International Journal of ISSI, Vol.10 (2013), No.1, pp. 27-33

# Welding of 304L Stainless Steel with Activated Tungsten Inert Gas Process (A-TIG)

E. Ahmadi[1*], A. R. Ebrahimi[2], R. Azari Khosroshahi[3]
[1,3]*Faculty of Material Engineering, Sahand University of Technology, Tabriz*
[2] *Department of Mining and Metallurgical Engineering, Amirkabir University of Technology, Tehran*

## Abstract

Gas tungsten arc welding is a popular process in those applications requiring a high degree of quality and accuracy. However, this process has a big disadvantage against the substantially high productivity welding procedures. Hence, many efforts have been made to improve its productivity. One of these efforts is the use of activating flux (A-TIG welding). In this study, the performance of A-TIG welding on 304L austenitic stainless steel plates has been presented. Two oxide fluxes, $TiO_2$ and $SiO_2$ were used to investigate the effect of A-TIG welding process on weld morphology, microstructure and mechanical properties of weldments. The experimental results indicated that A-TIG welding could increase the weld penetration and depth-to-wide ratio. It was also found that A-TIG welding could increase the delta-ferrite content of weld metals and improve the mechanical properties. Moreover, a 2D axial symmetric model was developed to simulate the flow behavior in the melting pool. These results were compared to those experiments carried out on a stainless steel (304L) melted by a stationary heat source.

*Keyword:* A-TIG welding, delta-ferrite, stainless steel, oxide flux.

## 1. Introduction

Gas–tungsten arc welding (GTAW), also called tungsten inert gas welding (TIG), is a process that melts and joins metals by heating them with an arc established between a non-consumable tungsten electrode and the metals[1)]. This process has been widely used in industry for its high weld quality, especially for stainless steel, titanium alloys and non-ferrous alloys. However, compared to other arc welding processes, such as gas metal arc welding (GMAW), plasma arc welding (PAW), or submerged arc welding (SAW), which have lower penetration, its productivity is relatively low[2)]. Therefore, in order to increase the TIG welding production, much research has been conducted since 1995. Pre-placing or brushing a thin layer of active flux consisting of oxides/or halides (A-TIG) on the plate before welding can significantly improve the weld penetration, as first proposed by the E.O. Paton Institute of Electric Welding in the 1960s[3-6)]. The United States Navy Joining Center has been successfully used in everyday production to reduce the cost and improve the quality of Navy ships and aircraft using A-TIG technique, which was developed by Edison Welding Institute. A-TIG technique makes it possible to intensify the conventional TIG practices for joining the thickness of 8-10 mm by single pass full penetration welds, with no edge preparation, instead of multipass procedures[7)]. In fact, the penetration capability is up to 300% compared with the conventional TIG welding process.

Although an agreed mechanism for increased A-TIG penetration has not been found yet, the current theory on the effect of activating flux on penetration is that the flux changes the surface tension in the weld pool so that the fluid flow is changed, thereby increasing the penetration[8,9)]. However, due to limited data available in the literature regarding the action of weld arc and the mechanisms that sustain this effect, this phenomenon requires further investigation. In the present work, two kinds of oxide powders were used to study the effect of activating flux on weld morphology, microstructure and mechanical properties in stainless steel 304L welds systematically. Moreover, in order to come to a basic understanding of mechanisms of penetration increase, together with the experimental investigation, a 2D axial symmetric model was developed using the finite element code to simulate the flow behavior in the weld pool.

## 2. Experimental procedure

### 2.1 Material and experimental conditions

A bead-on-plate weld was prepared on austenitic stainless steel 304L with chemical compositions listed in Table 1. Plates 6 mm in thickness were cut

**Corresponding author*
*Tel: +98 911 1770371* *Fax: +98 171 2260158*
*Email: e.ahmadiii@gmail.com*
*1.M.Sc Student*
*2. Associate Professor*
*3. Associate Professor*

into strips of 150 × 150 mm. Prior to the welding, the surface of the plate was roughly polished with 400 grit (silicon carbide) abrasive paper to remove all surface impurities and then cleaned by acetone. A direct current electrode negative (DCEN) polarity power source (DIGTIG PSQ 250) was used with a mechanized system in which the test piece moved at a constant speed under the torch. Activating flux, $SiO_2$ and $TiO_2$ were prepared in powder form, and then mixed with acetone, and a layer less than 0.2 mm thick was applied to the surface of the joint to be welded by means of a brush before TIG welding. Welding parameters used in the present work are given in Table 2. The samples were etched by a solution of 10 g $CuSO_4$ + 50ml HCl + 50ml $H_2O$ to reveal the weld shape. The cross-sections of the weld beads were photographed using an optical microscope (Olympus). Longitudinal tensile test, in accordance with ASTM-E8 and Vickers hardness tests under a load of 1.96 N for 15 s, was used to examine the metallurgical properties of A-TIG stainless steel welds.

*Table 1. Chemical composition of 304L austenitic stainless steel.*

| Element | C | Si | Mn | Ni | Cr | P | Co |
|---|---|---|---|---|---|---|---|
| (wt%) | 0.016 | 0.44 | 1.01 | 10.11 | 18.26 | 0.025 | 0.11 |

*Table 2. Welding parameters for TIG welding experiments.*

| | |
|---|---|
| Welding current | 180 A |
| Welding speed | 150 mm.s$^{-1}$ |
| Arc length | 3 mm |
| Tip angle of electrode | 75° |
| Shielded gas | Pure Argon |
| Gas flow rate | 13 L.min$^{-1}$ |
| Diameter of electrode | 3.2 mm |

### 2.2. Physical model and mathematical formulation model

In order to simplify the mathematical model, the following assumptions have been made: (1) the flow is Newtonian, incompressible, and homogeneous; (2) all of the physical properties of the liquid and solid metals are constant. The fluid flow was supposed to be laminar and driven by Marangoni, buoyancy and Lorentz forces. The heat source from the arc was assumed to have a Gaussian distribution on the top surface, as widely used in the literature. The free surface was supposed to remain flat. The numerical model solves the differential equations governing the conservation of mass (Eq.1), momentum (Eq.2-3) and energy (Eq. 5).

$$\nabla.\vec{\nu} = 0 \tag{1}$$

$$\rho(\frac{\partial \vec{\nu}}{\partial t} + \vec{\nu}.\nabla\vec{\nu}) = -\nabla p + \mu\nabla.(\nabla\vec{\nu} + (\nabla\vec{\nu})^t + F_v \tag{2}$$

$$F_v = \rho(1-\beta(T-T_{ref}))\vec{g} + \vec{J}\times\vec{B} \tag{3}$$

$F_v$ represents body forces in the weld pool; it is the sum of Lorentz force and buoyancy force. $\vec{\nu}$ is the velocity vector field in the weld pool, $t$ is time, $\rho$ is density, $\mu$ is viscosity, p is pressure field, g is gravity, $T_{ref}$ is a reference temperature taken as the solidus temperature of the alloy, $\vec{J}$ is the current density vector and $\vec{B}$ is the magnetic field vector.

According to equation 4, the equation of energy conservation could be written (Eq.5):

$$\begin{cases} f_L = 1, & \text{if } T > T_L \\ f_L = \dfrac{T-T_S}{T_L-T_S} & \text{if } T_S \le T \le T_L \end{cases} \tag{4}$$

$$f_L = 0 \quad \text{if } T < T_L$$

$$\rho C_P^{eq}(\frac{\partial T}{\partial t} + \vec{\nu}.\nabla T) = \nabla.(\lambda\nabla T) + Q \tag{5}$$

where $T$ is temperature, $C_p$ is specific heat and $C_P^{eq} = C_P + L_f(\partial f_L/\partial t)$ is an equivalent specific heat which takes into account the latent heat of fusion $L_f$.

Equations 6 and 7 correspond to the Gaussian energy distribution and the electric current applied on the sample surface, respectively.

$$Q_r = \frac{\eta IV}{2\pi R_S^2}\exp(-\frac{x^2}{2R_C^2}) \tag{6}$$

$$J_r = \frac{1}{2\pi R_C^2}\exp(-\frac{x^2}{2R_C^2}) \tag{7}$$

$$R_S = 0.047R_C \tag{8}$$

## 3. Results and discussion

### 3.1. The effect of flux on weld pool shape

The fusion zone shapes of the beads are shown in Figure 1 Based on the cross-sectional pictures, the dimensions and depth/width ratio of the fusion zone were calculated for all the experiment specimens. The increase in weld depth and the decrease in bead width were significant in the use of activating flux. It can also be seen in Fig. 1 that TIG welding with $SiO_2$ significantly increased the weld depth to bead width ratio (D/W). The D/W ratio of this weld was 1.03. The increase in penetration was enough to obtain full penetration welds in trials performed with a current as low as 180 A in 6 mm thick plates.

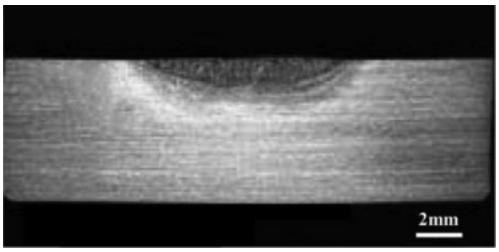


(a) Without Flux (D=1.61 mm, D/W=0.21).

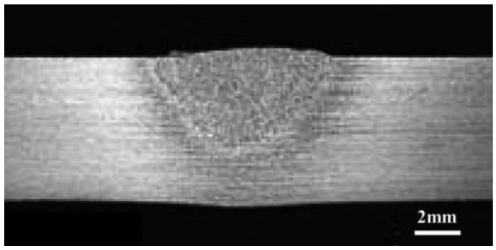


(b) With $TiO_2$ Flux (D=4.7 mm, D/W=0.68).

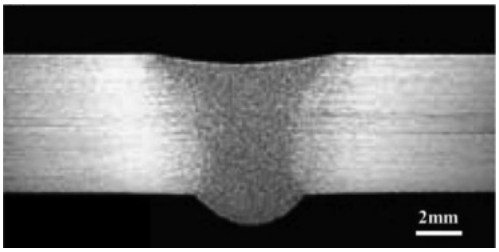


(c) With $SiO_2$ Flux (D=7.38 mm, D/W=1.03).

*Fig. 1. The effect of flux on weld pool shape.*

The driving forces for fluid flow in the GTA weld pools included the buoyancy forces, Lorentz forces, shear stresses induced by the surface tension gradient at the weld pool surface, and shear stresses acting on the pool surface due to the arc plasma as well as arc pressure. According to previous investigations, the surface tension gradient on the welding pool surface has been the principle factor that changes the fluid flow mode [10-14]. Generally, the surface tension is decreased with increasing temperature ($\partial\gamma/\partial T < 0$), for pure metal and many alloys. In this condition, the fluid flow of the molten pool surface is transferred easily from the pool center to the edge, and the weld pool shape is relatively wide and narrow as shown Figure 2(a). Heiple and Roper proposed that surface active elements such as oxygen, sulfur and selenium could change the temperature coefficient of the surface tension for iron alloys from negative to positive ($\partial\gamma/\partial T > 0$), and further influence the direction of the fluid flow in the weld pool as illustrated in Fig. 2(b). In that case, a relatively deep and narrow weld was produced [15].

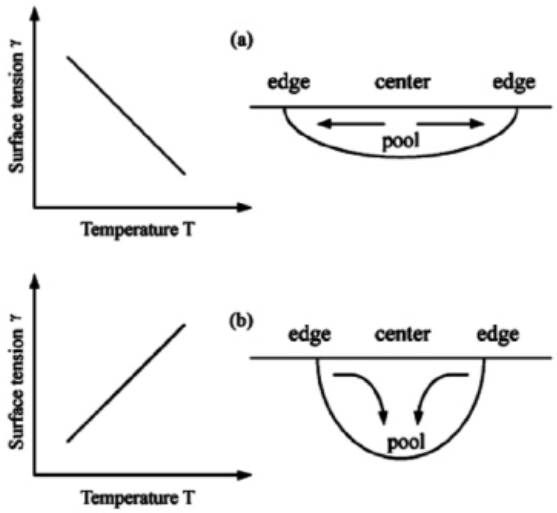


*Fig. 2. Marangoni convection mode in the weld pool: (a) $\partial\gamma/\partial T < 0$; (b) $\partial\gamma/\partial T > 0$.*

The other factor, which was due to the increase in weld penetration, was arc constriction. Because the conductivity of the flux was much lower than that of the metal vapors, and the melting and boiling points of the flux were higher than those of the weld metal, the metal evaporation would be only generated in the central regions of the welding arc, where the temperature was higher than the dissociation temperature of the flux compounds, thereby leading to a reduction in the conductivity area of the anode spot [16,17]. When using A-TIG welding, physically constricting the plasma column and reducing the anode spot tend to increase the energy density of the heat source and electromagnetic force of the weld pool, resulting in a relatively narrow and deep weld morphology compared with the conventional TIG welding. The simulation results for the distribution of electric current, magnetic field, Lorentz force and heat are shown in Figure 3 As can be seen, the Lorentz force can be considered as another factor in the increase of weld penetration.

Figure 4 presents the calculated velocities and the geometry of the weld beads obtained with a negative or positive surface tension gradient ($\partial\gamma/\partial T = \pm 5\times10^{-4}$) to simulate TIG and A-TIG welding. In this study, two parameters, arc efficiency $\eta = 75\%$ and heat distribution $R_C = 1.6$ mm, were considered. In this study, Lorentz forces were added or neglected to study their influence.

When the surface tension gradient is negative (TIG welding), if the electromagnetic forces are neglected, as expected, the liquid is pulled along the pool surface from the center to the edge, whereas with a positive surface tension gradient (A-TIG welding), the predominant flow is towards the heat source, resulting in a deeper and narrower weld pool shape. In that case, the dominant driving force is clearly the

Marangoni force as compared with the buoyancy force (Figure 3a, c). When Lorentz forces are taken into account, with a negative surface tension temperature gradient, two vortexes are observed. One vortex, being counterclockwise, is created by the electromagnetic force near the center of the weld pool; the other vortex, clockwise and very narrow, is located near the edge of weld pool caused by the surface tension effect. It can be observed that the flow is directed towards the axis in the vicinity of the heat source, but is directed away from the axis near the edge of the weld pool. As a result, the thermal energy from the arc is mainly carried inward, resulting in a deeper weld pool compared to the case without electromagnetic force, since in that case, there is nearly no flow at the center of the weld pool. However, the weld penetration obtained with a positive surface tension gradient is slightly higher when the electromagnetic force is neglected. It suggests that the magnitude of the velocities induced by the Lorentz force in the positive case is much smaller than that induced by the Marangoni force (Figure 3b, d). These qualitatively agree with previously published results [18-20]. Figure 5 shows the experimental and calculated shape of the cross section of TIG and A-TIG weld.

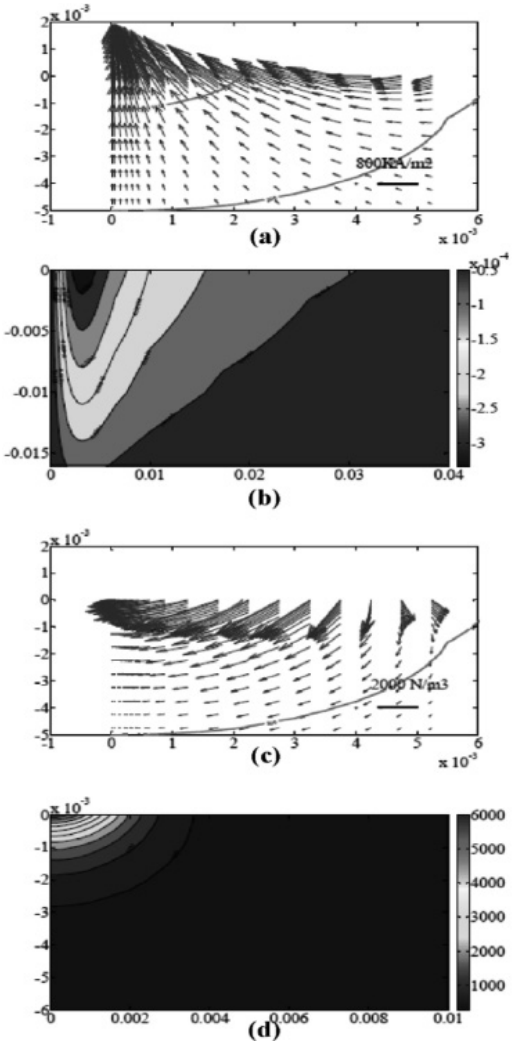


*Fig. 3. Distribution of (a) electric current, (b) magnetic field, (c) Lorentz force and (d) heat for TIG welding.*

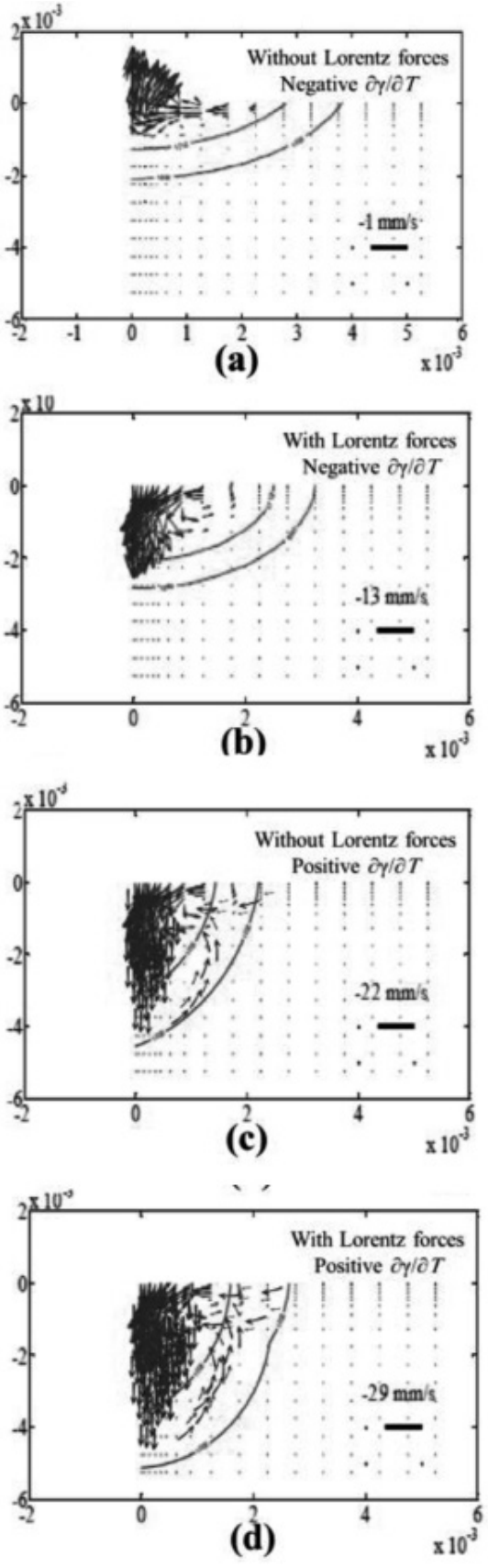


*Fig. 4. Distribution of the velocity field and Direction of fluid flow for ∂γ/∂T > 0 (a) without Lorentz force (b) with Lorentz force*

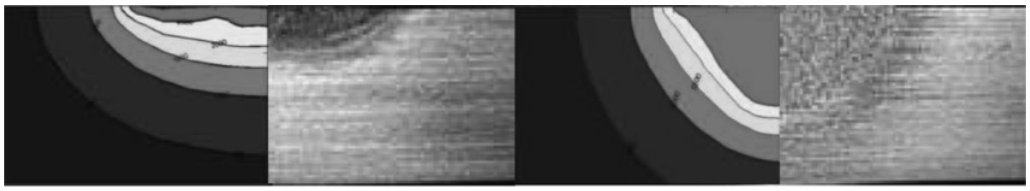


*Fig. 5. Calculated and exprimental shapes of the cross-section of the TIG weldment (a) without flux (b) with $TiO_2$ flux*

### 3.2. The effect of flux on microstructure

The experiments used 304L hot rolled stainless steel plate as a base metal. The ferrite number (FN) was measured using a calibrating magnetic instrument with a FERITSCOPE MP30. Figure 6 shows the microstructure and measured delta-ferrite content in 304L stainless steel weld metal produced with and without flux. The weld metal presented an austenite and δ-ferrite structure and the structure of the weld metal was completely different from that of the base metal. Previous research has shown that the microstructure of the 304L stainless steel mainly consists of austenite (γ) under equilibrium solidification. However, during the non-equilibrium rapid solidification, the high cooling rate resulted in incomplete δ/γ transformation and some metastable δ-ferrite unavoidably remained [21-23]. Therefore, more delta-ferrite was retained in the weld metal after solidification.

In Type 304L stainless steel TIG welds produced without flux, the delta-ferrite content was increased to 6.2 FN from its initial value of 1.3 FN. On the other hand, when using activating fluxes, the delta-ferrite content in the activated TIG weld metal was slightly increased to 7.0 and 7.4 FN for $TiO_2$ and $SiO_2$, respectively. This is related to the heat input during TIG welding with and without flux. It is well known that the variation in heat input can significantly affect the microstructure [24, 25]. The experiment results showed that for the constant value of weld current, by using the activating flux, arc voltage was increased from 14.1 to 16-16.3V due to "arc constriction". Since the calculated heat input is proportional to the measured arc voltage, applied activated flux has the positive effect of increasing the heat input unit length of welds. Therefore, this higher heat input can increase the peak temperature of the welds, and more delta-ferrite is formed in the activated TIG weld metal.

### 3.3. The effect of flux on mechanical properties

Figure 7 presents the experimental results for the mechanical properties of TIG weldment with and without and activating fluxes. It can be clearly seen that the weldment obtained by using TIG welding with the activating flux exhibited better-mechanical properties (including ultimate tensile strength, elongation, and hardness) than those of TIG weldment without using the activating flux. The austenite had a cubic face-centered (FCC) crystal structure. The delta-ferrite has a body-centered cubic (BCC) crystal structure.

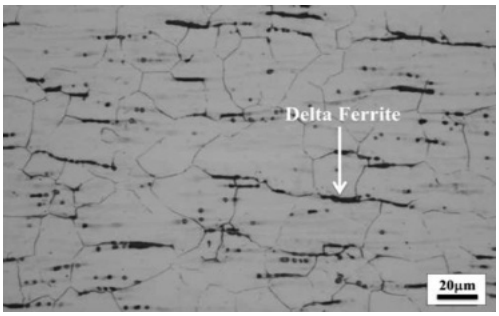


(a)

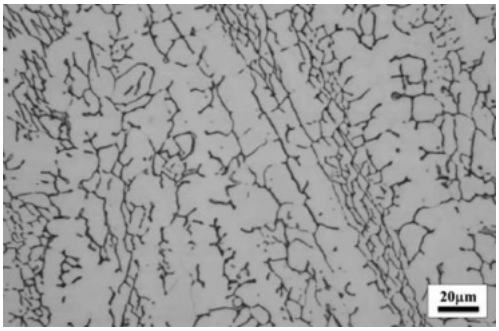


(b)

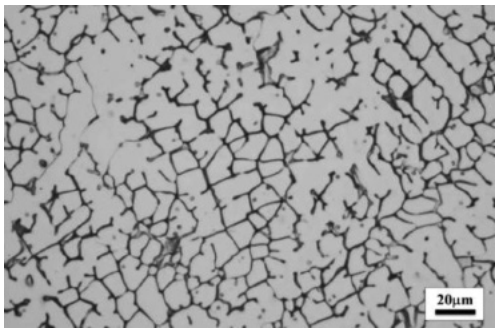


(c)

*Fig. 6. Optical micrograph of microstructure in (a) 304L base metal (b) fusion zone without flux (c) with $SiO_2$ flux.*

The BCC structure had a mechanical strength higher than that of the FCC structure. When TIG welding with activating flux was used, the delta-ferrite content in the weld metals was increased, showing a beneficial effect in increasing the mechanical properties of type 304L stainless steel welds. In addition, this may be attributed to the better desulphating and deoxidizing ability of activating fluxes. Due to this advantage of flux, the shape and distribution of inclusion existing in welding can be improved, thus improving the performance of the welded structure.

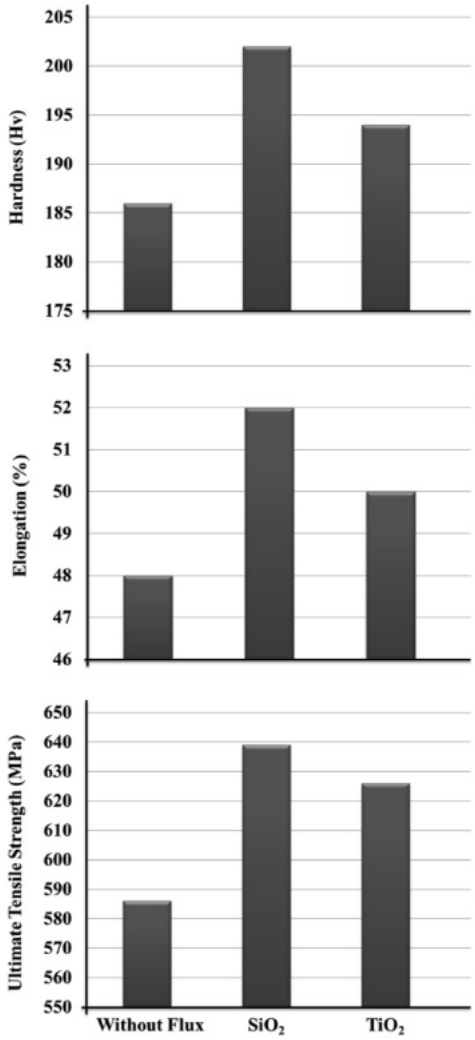


*Fig. 7. The effect of activating flux on the mechanical properties*

## 4. Conclusion

1. The addition of an activating flux led to an increase in the penetration depth and a decrease of the width.
2. Simulations showed the Marangoni effect combined with Lorentz forces in TIG and A-TIG welding processes.
3. The results of experiments agreed with the simulation conducted for TIG welding.
4. A-TIG welding could increase retained delta ferrite of the weld metal.
5. A-TIG weldment exhibited mechanical properties (including strength, ductility, and hardness) better than those of TIG welding without flux.

## References

[1] S. Kou, Welding metallurgy: LibreDigital, 2003.
[2] A. H. Kokabi, P. Farhang, A. Adab Avazeh: welding dictionary, 1th Eddition, Azadeh, (2004).
[3] C. Dong, S. Katayama:The 57th Annual Assembly of the International Institute of Welding, Osaka, (2004), 371.
[4] S. MARYA: Mech. Mater. Eng., 1(2006), 1.
[5] P. J. Modenesi, E. R. Apolinario, I. M. Pereira: J. Mater. Sci. Technol, 99(2000), 260.
[6] M. M. Sawickij, G. M. Mielniczuk, A. F. Lupan, A. M. Sawickij: Weld. Int., 15(2001), 677.
[7] D. S. Howes and W. Lucas: Weld. Met. Fabr, Vol. 68, pp. 11-17, 2000.
[8] Chern, T.S., Tseng, K.H., Tsai, H.L, "Study of the characteristics of duplex stainless steel activated tungsten inert gas welds", Materials and Design, Vol. 32, pp. 255-263, 2011.
[9] T. Sándor, J. Dobránszky, "The experiences of activated tungsten inert gas (ATIG) welding applied on 1.4301 type stainless steel plates,", Vol. 3, pp. 63-70, 2007.
[10] Ch. Yang, S. Lin, F. Liu, Q. Zhang, "Reaserch on the mechanism of penetration increase by flux in A-TIG welding", Material Science and Technology, Vol. 19, pp. 225-227, 2003.
[11] Sh. Lu, H. Fuji, H. Sugiyama, K. Nogi, "Mechanism and Optimization of Oxide Fluxes for Deep Penetration in Gas Tungsten Arc Welding", Metallurgical and Materials Transactions A, Vol. 34, pp. 1901-1907, 2003.
[12] J. J. Lowke, M. Tanaka, M. Ushio, "Mechanisms giving increased weld depth due to a flux", Physics D: Applied physics, Vol. 38, pp. 3438-3445, 2005.
[13] M. M. Sawickij, G. M. Mielniczuk, A. F. Lupan, A. M. Sawickij, O. I. Olejnik, "Activating fluxes in inert gas-shield welding of steels", Welding International, Vol. 15, pp. 677-683, 2010.
[14] S. Leconte, P. Paillard, P. Chapelle, G. Henrion, J. Saindrenan, " Effects of flux containing fluorides on TIG welding process", Science and Technology of Welding and Joining, Vol. 12, pp. 120-126, 2007.
[15] S. Lu, H. Fujii, K. Nogi, "Marangoni convection and welding penetration in A-TIG welding", Theoretical and Applied Fracture Mechanics, Vol. 48, pp. 178-186, 2007.
[16] L. Qing-ming, W. X. Hong, Z. Zeng, W. Jun, "Effect of activating flux on arc shape and arc voltage in tungsten inert gas welding," Transactions of Nonferrous Metals Society of China, vol. 17, pp. 486-490, 2007.
[17] Y. Ogawa, "Effect of active flux on anode

reaction", Document XII-1797-04, National Institute of Advanced Industrial Science and Technology, Japan.
[18] Y. Wang, Q. Shi, H. L. Tsai, "Modeling of the Effects of Surface-Active Elements on Flow Patterns and Weld Penetration", Metallurgial and Materials Transaction B, Vol. 32, pp. 145-161, 2001.
[19] A. Traidia, F.Roger, E. Guyot, "Optimal parameters for pulsed gas tungsten arc welding in partially and fully penetrated weld pools", Thermal Sciences, Vol. 49, pp. 1197-1208, 2010.
[20] R. Zhang and D. Fan, "Numerical simulation of effects of activating flux on flow patterns and weld penetration in ATIG welding," Science and Technology of Welding & Joining, vol. 12, pp. 15-23, 2007.
[21] K. Prasad Rao, A. Uma Maheshwar Rao, G. J. Gururaja, "Effect of delta ferrite content on the corrosion resistance of type 316 clad metals", Materials and Corrosion, Vol. 39, pp. 135-142, 1988.
[22] J. C. Lippold, D. J. Kotecki, "Welding metallurgy and weldability of stainless steels", Wiley Interscience; 1 edition, ISBN 9780471473794, 2005.
[23] V. Shankar, T. P. Gill, S. L. Mannan, "Solidification cracking in austenitic stainless steel welds", Sadhana, Vol. 28, pp. 359-382, 2003.
[24] P. Sejč, R. Kubíček, "Influence of Heat Input on the Content of Delta Ferrite in the Structure of 304L Stainless Steel GTA Welded Joints", Scientific Proceedings Faculty of Mechanical Engineering STU in Bratislava, Vol. 19, pp. 8-14, 2012.
[25] R. J. Fowless, S. E. Blake, "Influence of Heat Input on Austenitic Stainless Steel Weld properties", African fusion, Vol. 1, pp. 17-24, 2008.
[26] A. Rodrigues, A. Loureiro, A. C. Batista, "Phase formation in austenitic stainless steel A-TIG welds", Materials Science Forum, Vol. 514/516, pp. 549-553, 2006.